NEURAL REGENERATION RESEARCH
February 2015, Volume 10, Issue 2
www.nrronline.org

RESEARCH ARTICLE

Brain functional network connectivity based on a visual task: visual information processing-related brain regions are significantly activated in the task state

Yan-li Yang, Hong-xia Deng, Gui-yang Xing, Xiao-luan Xia, Hai-fang Li*

School of Computer Science and Technology, Taiyuan University of Technology, Taiyuan, Shanxi Province, China

***Correspondence to:**
Hai-fang Li, Ph.D.,
lihaifang@tyut.edu.cn.

***doi:**10.4103/1673-5374.152386*
***http:**//www.nrronline.org/*

***Accepted:** 2014-12-17*

Abstract

It is not clear whether the method used in functional brain-network related research can be applied to explore the feature binding mechanism of visual perception. In this study, we investigated feature binding of color and shape in visual perception. Functional magnetic resonance imaging data were collected from 38 healthy volunteers at rest and while performing a visual perception task to construct brain networks active during resting and task states. Results showed that brain regions involved in visual information processing were obviously activated during the task. The components were partitioned using a greedy algorithm, indicating the visual network existed during the resting state. *Z*-values in the vision-related brain regions were calculated, confirming the dynamic balance of the brain network. Connectivity between brain regions was determined, and the result showed that occipital and lingual gyri were stable brain regions in the visual system network, the parietal lobe played a very important role in the binding process of color features and shape features, and the fusiform and inferior temporal gyri were crucial for processing color and shape information. Experimental findings indicate that understanding visual feature binding and cognitive processes will help establish computational models of vision, improve image recognition technology, and provide a new theoretical mechanism for feature binding in visual perception.

***Key Words:** nerve regeneration; functional magnetic resonance imaging; resting state; task state; brain network; module division; feature binding; Fisher's Z transform; connectivity; visual stimuli; NSFC grants; neural regeneration*

***Funding:** This study was financially supported by grants from the National Natural Science Foundation of China, No. 61170136, 61373101, 61472270, and 61402318; Natural Science Foundation (Youth Science and Technology Research Foundation) of Shanxi Province, No. 2014021022-5; Shanxi Provincial Key Science and Technology Projects (Agriculture), No. 20130311037-4.*

Yang YL, Deng HX, Xing GY, Xia XL, Li HF (2015) Brain functional network connectivity based on a visual task: visual information processing-related brain regions are significantly activated in the task state. Neural Regen Res 10(2):298-307.

Introduction

Functional magnetic resonance imaging (fMRI) has been widely used in the field of modern neuroscience, especially cognitive neuroscience. Many of these studies focus on functional brain networks (Liang et al., 2012; Song et al., 2012; Yu et al., 2012; Seo et al., 2013). Previous studies have demonstrated that brain networks are not only involved in motor function, but are also correlated with vision, audition, and language (Yuan et al., 2013).

Increasingly, research into feature binding in visual perception has focused on using fMRI to find brain regions activated by different types of visual stimuli. The functional architecture of the visual pathway for object recognition in the human brain has been investigated using functional magnetic resonance imaging to measure patterns of responses in ventral temporal cortex while subjects viewed faces, cats, five categories of man-made objects, and nonsense pictures. The results indicated that the representations of faces and objects in ventral temporal cortex are widely distributed and overlapping (Haxby et al., 2001). Studies have also demonstrated that extrastriate visual cortical areas are relatively sensitive to images of hands (Bracci et al., 2010). The parahippocampal gyrus, lateral occipital complex, and cingulate cortex have been shown to be highly involved in the classification of natural scenery (Walther et al., 2009). After subjects were subjected to visual stimuli with alternating object features (color, shape, texture), color and texture were shown to be processed in medial temporal and occipital cortices, while geometric features were processed in lateral temporal and occipital cortices (Cavina-Pratesi et al., 2010).

Several methods have arisen to study complex brain networks, and the graph-theory approach is the most commonly used. Among the graph theories, community struc-

ture and community detection have been widely viewed as important. The module structure of functional brain networks in animals and humans was explored using graph theory (Hilgetag et al., 2000; Ferrarini et al., 2009; Meunier et al., 2009).

Researchers have also used a hierarchical clustering method to detect similarities in low-frequency fluctuations. They investigated the contribution of motion and hardware instabilities to resting-state correlations and provided a method to reduce artifacts. For all cortical regions studied and clusters obtained, they quantified the degree that functional connectivity maps were contaminated by respiration and heart beats. Results indicated that patterns of functional connectivity can be obtained with hierarchical clustering that resembles known neuronal connections (Cordes et al., 2002). Meunier et al. (2009) investigated the modular structure of these networks in two groups of healthy participants (young and older) and tested the hypothesis that normal brain aging might be associated with changes in modularity of sparse networks. Newman's modularity metric was maximized and topological roles were assigned to brain regions depending on their specific contributions to intra- and inter-modular connectivity. Both young and older brain networks demonstrated significantly non-random modularity. He et al. (2009) found the resting-state functional brain network has typical modularization properties. The whole brain can be divided into six modules, including somatosensory/motor, auditory, attention, visual, subcortical, and the "default" system. Further study found that there exists a certain point between modules and the connection to ensure that the network connectivity and stability.

Here, in an attempt to explore visual feature binding, assist computer modeling, and provide evidence for an objective assessment of optic nerve regeneration and repair after injury, we constructed a resting-state functional brain network using resting-state and task-state fMRI data of 36 subjects, and analyzed the connectivity of brain regions and the module partition of the constructed brain network.

Participants and Methods

Participants

Thirty-eight healthy volunteers were enlisted through responses to an advertisement. Two cases were excluded because of head movement greater than 3 mm or 3° of rotation. Thus, 36 cases (19 females; 17 males; mean age 26.8 years; range, 17–51 years) were included in the study.

The criteria for inclusion were: absence of color blindness; no history of organic lesions in either eye; normal visual acuity or corrected visual acuity; absence of other specific diseases or mental disorders; and no metallic implants. All subjects volunteered to participate in the experiments and gave informed consent.

fMRI data acquisition

Structural and functional images were acquired using an Achieva 1.5T ND MRI system (Philips, the Netherlands). Visual stimuli were presented using E-Prime 2.0 software. Images (7 degrees in visual angle) were presented onto a screen *via* a projector and then reflected through a mirror for subjects to view while in the scanner. Structural imaging: axial T1 sequence, slice thickness = 3.59 mm, whole-brain scans, 28 slices. Functional imaging adopted a single shot echo-planar imaging sequence and scan parameters were as follows: field of view = 230 mm × 230 mm, repetition time = 2,000 ms, echo time = 31 ms, flip angle = 90°, slice thickness = 3.59 mm, matrix = 64 × 64. The orientation during functional imaging was similar to that during structural imaging. During scanning, subjects were kept conscious, clear headed, and stationary. They were asked to fixate on the center of the images to ensure that the position of retina stimulation was fixed. The effect of ambient light on the subjects was minimized, with all light sources in the room turned off except for the MRI projector.

fMRI data preprocessing

Data preprocessing was performed using SPM8 software (http://www.fil.ion.ucl.ac.uk/spm). Data sets were subjected to tome-slice and motion correction, with head motion limited to less than 3 mm or 3°. The corrected images were optimized by a 12-dimensional affine transformation and conformed to MNI standard space with 3-mm voxels. Finally, images were smoothed by low frequency filtering (0.06–0.11 Hz) to reduce low-frequency drift and high-frequency biological noise.

Construction of brain function network

To study how the brain works during visual tasks, connectivity, and module partition of functional brain networks in the resting state, the brain was divided into 90 brain regions (45 in each hemisphere) using the anatomical automatic labeling (AAL) template (Tzourio-Mazoyer et al., 2002), and each brain region was defined as a node in the network. The average time sequence of all voxels in the same brain region was calculated as the time series of this region. The number of connection lines in the network was defined using the partial correlation coefficient. The time sequence of each brain region was obtained and subject to multivariate linear regression to remove the influence of covariant. Then the partial correlation coefficients between any two regions were calculated and a 90 × 90 incidence matrix was obtained (Guo et al., 2014).

fMRI data obtained during the task and resting states was used to determine the time series correlation matrix for each subject, and then averaged. The resting-state and task-state functional brain networks (90 × 90) were constructed. Accordingly, functional brain mechanisms underlying the visual binding state were explored and lay the foundation for partition of modules in the brain function network.

Fisher's *Z* transformation

Connectivity coefficients represent the functional connectivity between two nodes in the brain-function network and determine the degree of network connectivity.

To make the connectivity coefficients accord with normal distributed, it should be accomplished with a Fisher's *Z*

transformation. The resultant Z values indicate relative connectivity, with higher Z values indicating closer connectivity between two nodes. The Z values were calculated using the following formula (the Fisher's Z transformation):

$$Z = \frac{1}{2} ln \frac{1+r}{1-r} \quad (1)$$

where r represents the coefficient of correlation.

Connectivity analysis

Connectivity is a useful attribute of complex networks, representing the total number of active connections to a given node and further evidencing the importance of that node in the network. The degree of connectivity uses the coefficient of correlation:

$$\eta_{ij} = e^{-\xi d_{ij}} \quad (2)$$

where ξ is a constant indicating variation of connectivity between two nodes and represents the distance between two nodes. It is calculated according to the following formula:

$$d_{ij} = (1 - r_{ij})/(1 + r_{ij}) \quad (3)$$

Here r_{ij} is the coefficient of correlation between two nodes. At any node in the network, the sum of the connectivity degrees between that node and all other nodes in the network was the total connectivity at that node:

$$\Gamma_i = \Sigma_{j=1}^{n} \eta_{ij} \quad (4)$$

After standardization, the formula is modified to:

$$\Gamma_i = \Gamma_i \Big/ \Sigma_{j=1}^{n} \Gamma_j \quad (5)$$

Module partition of the brain-function network

There are two algorithms for partitioning the brain-function network: optimization-based and heuristic. Optimization-based methods include the spectral method (White and Smyth, 2005), the Kernighan-Lin algorithm (Newman, 2004a), and the fast Newman algorithm (Newman, 2004b). The fast Newman algorithm is the modularity-based (also known as Q-function) optimization method that was proposed by Newman in 2004 (Newman and Girvan, 2004), but it is not appropriate for large-scale complex networks. Subsequently, Clauset, Newman, and Moore modified the fast Newman algorithm using heap structure (Clauset et al., 2004) and named it the CNM algorithm. The complexity of the CNM algorithm was close to linear and is appropriate for large-scale, complex networks. Therefore, a greedy algorithm (CNM algorithm) based on the modularity of heap structure was used for module partition. Module partition is usually characterized by tight connection within a module and sparse connection between modules.

Modularity is a sensitive indicator of module partition:

$$Q = \frac{1}{2m} \left(\sum_r e_{rr} - \frac{a_r^2}{2m} \right) \quad (6)$$

where e_{rr} is the number of the lines within module r, and

$$a_r = \sum_s e_{rs} \quad (7)$$

indicates the lines from the nodes within module r,

$$2m = \sum_r a_r = \sum_{rs} e_{rs} \quad (8)$$

CNM algorithm

Three data structures were used, including the modularity incremental matrix ΔQ_{ij}, the maximum heap H, and vector a_i. The algorithms are as follows:

(1) Data initialization. Modularity incremental matrix was defined as:

$$\Delta Q_{ij} = \begin{cases} 1/2m + k_i k_j / (2m)^2, & \text{community } i \text{ connected with } j \\ 0, & \text{other} \end{cases} \quad (9)$$

where k_i is the degree of community i, and m is the total number of the lines in the network.

$$a_i = k_i / 2m \quad (10)$$

The initial matrix ΔQ_{ij} and vector a_i were calculated and the value of the maximum element in each row of matrix ΔQ was stored using the maximum heap H.

(2) Combine community i with community j.

The maximal ΔQ_{ij} was selected from the maximum heap H, and community i was combined with community j to form community ij. The module incremental matrix was changed to ΔQ_{ij} and auxiliary vector .

(3) Repeat step (2), until the Q value remained unchanged. At this time, the algorithm was terminated and the maximum Q value was obtained.

Statistical analysis

Data were preprocessed using statistical parametric mapping software (SPM8, http://www.fil.ion.ucl.ac.uk/spm). For statistical parametric mapping, the correlation between hemodynamic responses of each voxel and the experimental design was estimated using generalized linear models, and task-related brain activity was detected using a two-sample t-test (FDR correction, $P < 0.05$, cluster size ≥ 10 voxels).

Results

Visual stimulation task

Each stimulus had two features: color and shape. We used three primary colors (red, green, and blue) and three shapes (circle, square, and triangle).

Experimental paradigm 1: Stimuli were combined into four possibilities (**Figure 1**): (1) same shape and same color (**Figure 1A**), (2) same color, but different shapes (**Figure 1B**), (3) same shape but no color (**Figure 1C**), or (4) same shape but different colors (**Figure 1D**). Subjects selected the number (1, 2, 3, or 4) corresponding to the combination by

Table 1 Brain regions activated more in experimental paradigm 1 than in control tasks

Brain region	Hemisphere	Brodmann area	Activated regions	Talairach coordinate (mm)			*Z* value	*T* value
				X	*Y*	*Z*		
Cuneus	L	18	260	−6	−90	10	Infinite	9.02
		19		−12	−93	27	7.58	8.07
		19		−33	−87	12	5.32	5.49
Lingual gyrus	R	17	121	15	−90	−6	7.51	8.00
		17		12	−102	21	7.10	7.50
		19		21	−93	24	4.94	5.08
Middle frontal gyrus	R	6	100	33	−6	66	6.70	7.04
		6		30	−3	51	5.76	5.98
Precuneus	R	7	23	21	−78	54	6.09	6.34
Middle temporal gyrus	R	19	15	39	−81	15	5.94	6.17
Middle frontal gyrus	R	46	30	45	24	27	5.89	6.12
Inferior temporal gyrus	L	19	19	−48	−75	−3	5.54	5.73
Fusiform gyrus	L	37	11	−42	−69	−12	5.48	5.67

The activated brain regions were analyzed using SPM8 software (FDR correction, $P < 0.05$, cluster size ≥ 10 voxels). *Z* value is the statistical transformation value in the *t*-test, higher *Z* value indicates more significant difference. L: Left; R: right.

Table 2 Brain regions activated more in experimental paradigm 2 than in control tasks

Brain region	Hemisphere	Brodmann area	Activated regions	Talairach coordinate (mm)			*Z* value	*T* value
				X	*Y*	*Z*		
Cuneus	L	18	1,542	−15	−93	33	Infinite	10.99
	L	18		−18	−90	21	Infinite	8.43
	R	17		21	−93	21	7.5755	8.07
Frontal gyrus	L	6	61	−15	−9	78	6.8182	7.17
	L	6		−15	−76	60	6.5431	6.86
	L	6		−12	−6	69	6.4834	6.79
Middle frontal gyrus	R	9	40	42	18	27	6.0531	6.30
Cingulate cortex	L	24	19	0	21	6	5.7854	6.00
Frontal gyrus	R	6	78	33	−6	69	5.7805	6.00
Frontal gyrus	R	6	45	27	0	60	5.7181	5.93
Cingulate gyrus	R	24	46	18	0	51	5.5511	5.74
Anterior gingulate	L	24	27	−18	33	9	5.682	5.89
Fusiform gyrus	L	37	11	−42	−69	−12	5.48	5.67

The activated brain regions were analyzed using SPM8 software (FDR correction, $P < 0.05$, cluster size ≥ 10 voxels). *Z* value is the statistical transformation value in the *t*-test, higher *Z* value indicates more significant difference. L: Left; R: right.

pressing one of four buttons.

Experimental paradigm 2: Find the test image having the same features as the target image (**Figure 1E–H**). Each stimulus consisted of two rows. The top row contained a single target stimulus, and the bottom row contained an array of four test stimuli. Target stimuli and the stimuli were compared using different combinations of features. Subjects selected the matching stimulus by pressing a corresponding button (**Figure 1E–H**).

The task procedure is shown in **Figure 2**. First, subjects fixated on a central cross for 4 seconds. Next, the stimuli were presented for 4 seconds. Then, instructions for the button response were presented until a response was made. After the selection was made, the phrase "please wait" was presented on the screen. The time from instruction onset until the start of the next trial was always 8 seconds, ensuring that each trial lasted 16 seconds. Each combination was pseudorandomly presented 8 times for a total of 32 trials, making the time for each experimental task 512 seconds.

Position of data activation regions

Brodmann area (BA) partitions were defined by Korbinian Brodmann according to the cellular structure of cortical tissue as viewed under a light microscope. There are 52 BAs and the position analysis was performed using them as the template.

Experimental paradigm 1

Data were collected and brain regions more active in visual perception were identified using the task-rest contrast (**Table 1**). The regions significantly more active in the task condition were: occipital lobe (BA17, 18, 19), middle and inferior temporal gyrus (BA37), right anterior central gyrus (BA6), superior and middle frontal gyrus (BA46), and parietal lobe (BA7). The most obvious activation occurred in the

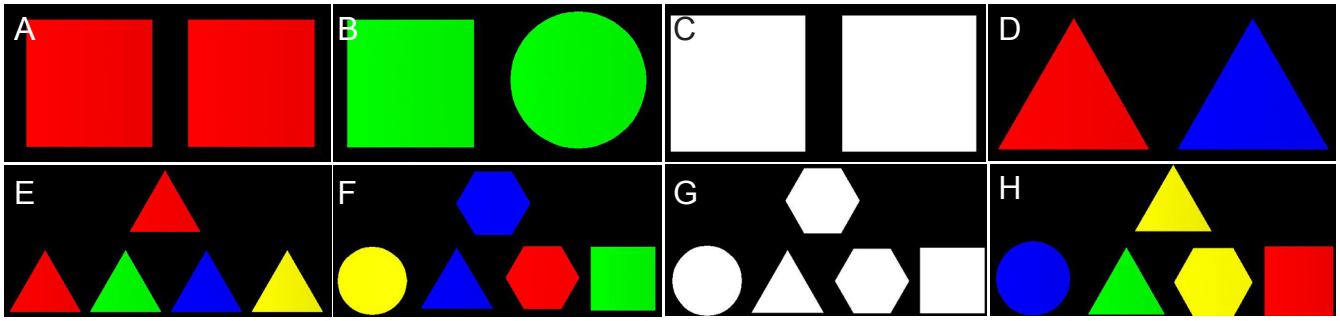

Figure 1 Experimental paradigms 1 (A–D) and 2 (E–H).
(A, E) Same color and same shape. (B, F) Same color but different shapes. (C, G) Same shape and no color. (D, H) Same shape but different colors.

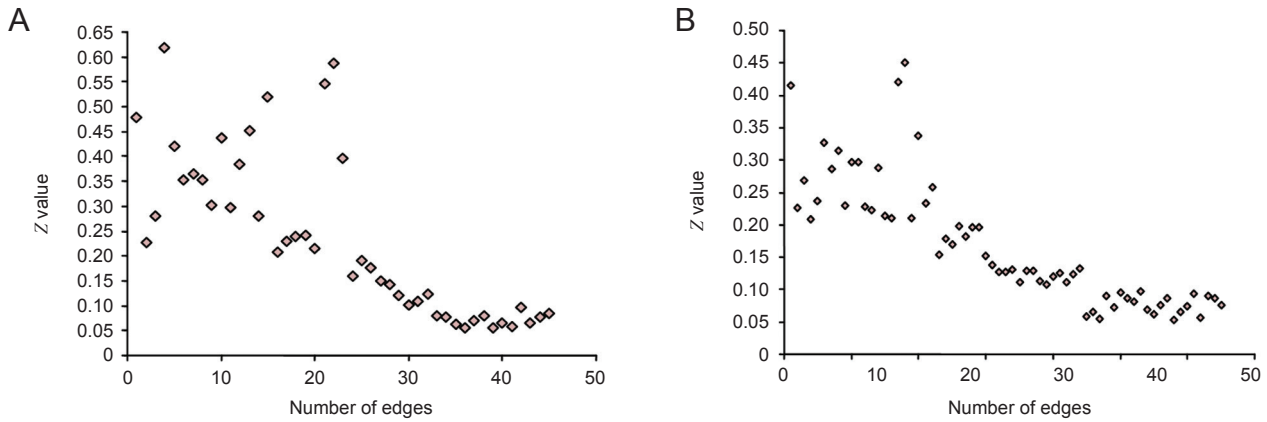

Figure 4 *Z*-values of the transformed correlation coefficients at visual brain regions.
(A) Resting state (n=45). (B) Task state (n=65). When subjects were in a t-test, 18 brain regions containing 162 lines were involved in visual information processing. After transformed Z-values were analyzed using the t-test, 84 positive connections were found. When subjects viewed stimuli with different color and shape features, 18 brain regions containing 162 lines were involved in the visual information processing. After Z-values were analyzed using a t-test, 86 positive connections were found.

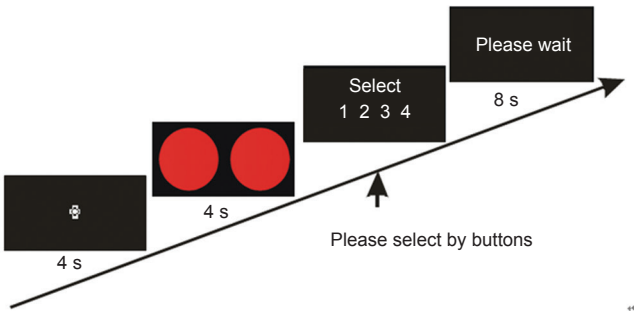

Figure 2 Stimulus presentation process.
First, subjects fixate the cross for 4 seconds. Then stimuli appear for 4 seconds, followed by instructions asking subjects to select the number representing the combination by pressing one of four buttons. The numbers represented (1) same color, same shape, (2) same color, different shapes, (3) same shape, no color; and (4) same shape, different colors. Next, subjects wait until the next trial. s: Seconds

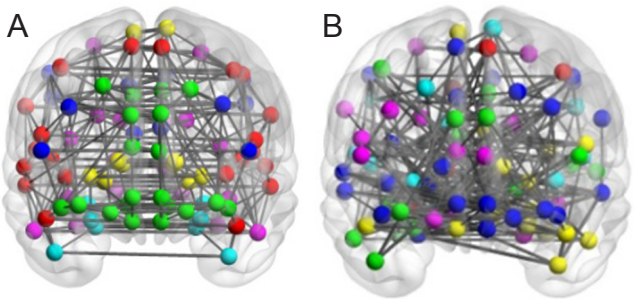

Figure 6 The connection map of resting-state and task-state brain-function networks.
(A) The resting-state network was divided into six modules. (B) The task-state network was divided into seven modules. Thicker lines represent stronger correlation between the two brain regions. Nodes with the same color are located in the same module.

lingual gyrus (BA18). The brain regions were active in the double-feature (color and shape) and the control conditions, included occipital lobe (BA17, 18, 19). In single-feature and control conditions, the occipital lobe (BA17, 18, 19) was significantly activated. The shape-color contrast revealed significantly more activation in the left occipital visual association (BA18). The color-shape contrast revealed significantly more activation in the fusiform gyrus (BA37).

Experimental paradigm 2

Data were collected and brain regions more active in visual perception were identified using the task-rest contrast (**Table 2**). The regions significantly more activate in the task condition were: occipital lobe (BA17, 18, 19), middle and

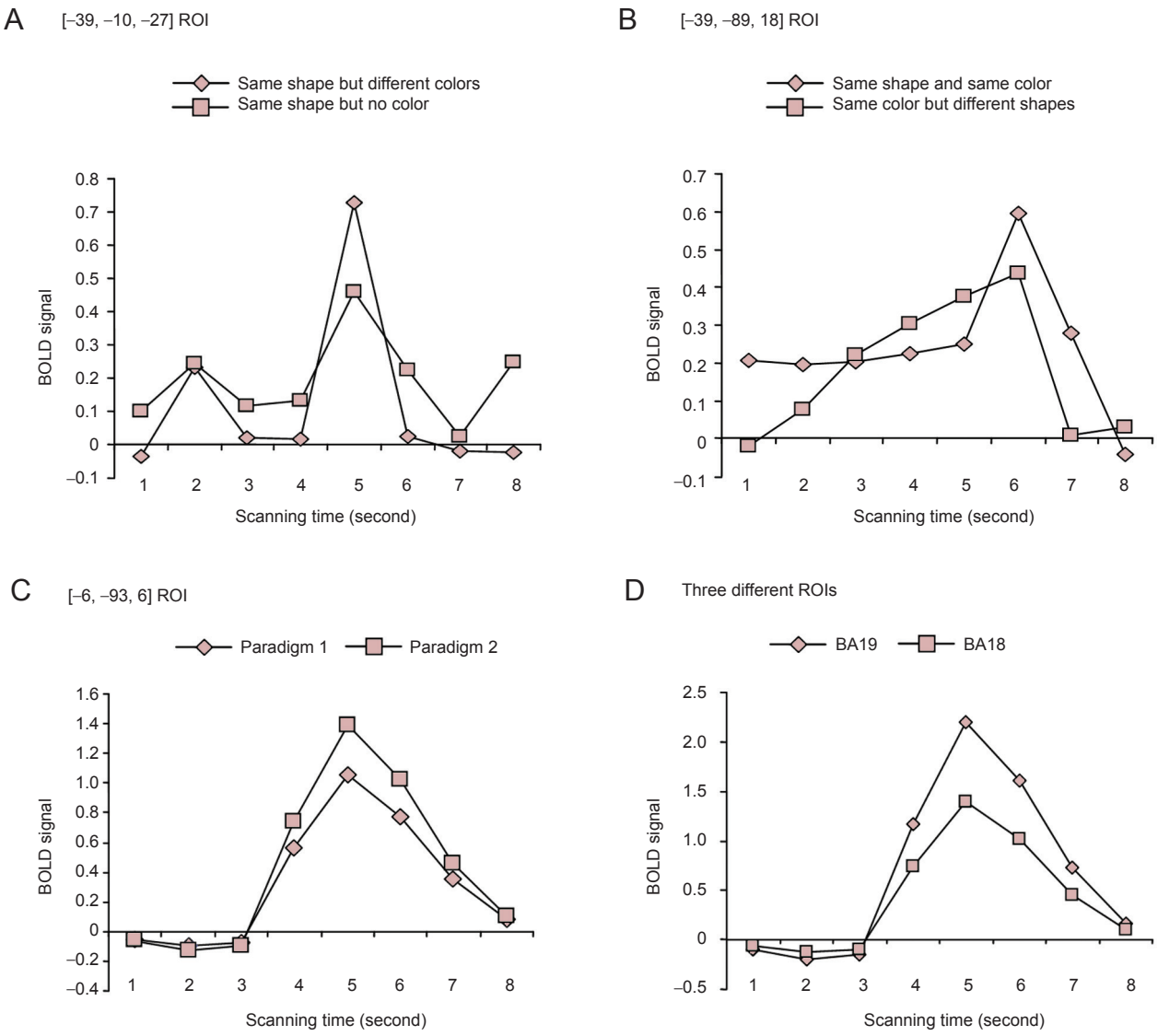

Figure 3 fMRI signals at ROI.
(A) Comparing two task conditions showed that peak BOLD signals were higher when processing different colors. (B) Comparing two task conditions showed that BOLD signals exhibited a wide response width when processing different shapes. (C) Comparing complex tasks with simple tasks showed that peak BOLD were higher during complex tasks. (D) BA18 was activated less than BA19 during the complex task. fMRI: Functional magnetic resonance imaging; ROI: region of interest; BOLD: blood oxygenation level dependent; BA: Brodmann area.

inferior temporal gyrus (BA37), right anterior central gyrus (BA6), superior and middle frontal gyrus (BA46), prefrontal cortex (BA9), parietal lobe (BA7), cingulate gyrus (BA31), and surrounding cingulate cortex (BA24). Experimental paradigm 2 significantly enhanced the activation in the lingual gyrus (BA18). The double-feature condition activated occipital lobe (BA17, 18, 19), right anterior central gyrus (BA6), parietal lobe (BA7), and cingulate cortex (BA24) more than the control condition did. The single-feature condition activated the occipital lobe (BA17, 18, 19) significantly more than the control condition did. In this task, BA46 was also activated because of working memory (*i.e.*, short-term memory) and attentional requirements of the task. BA7, which is highly involved in the integration of visual spatial information and receives projections from the corpus striatum and cingulate gyrus, was also activated.

According to the Talairach coordinates [–39, –10, –27], a region of interest (ROI) in the fusiform gyrus was selected. The blood oxygenation level dependent (BOLD) signals are shown in **Figure 3A**. Comparing the two task conditions revealed that peak BOLD signals were high when processing different colors, which was consistent with studies addressing the correlation between fusiform gyrus activity and color. According to the Talairach coordinates [–39, –89, 18], a ROI in the visual association cortex BA18 was selected and the BOLD signals are shown in **Figure 3B**. Comparing the two task conditions revealed that these BOLD signals exhibited a wide response width upon processing different shapes.

According to the Talairach coordinates [–6, –93, 6], a ROI in visual association cortex BA18 was selected and the BOLD signals are shown in **Figure 3C**. Comparing paradigm 1 (simple) and paradigm 2 (complex) showed that peak

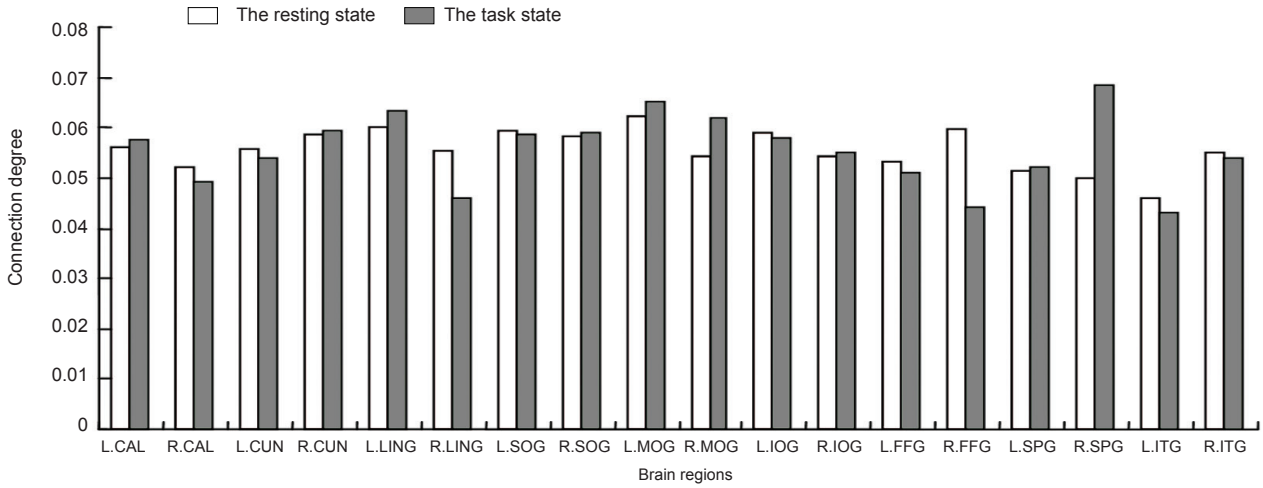

Figure 5 Connectivity between visual brain regions.
When subjects were at rest, connectivity was the highest in the left middle occipital gyrus (0.0621), followed by the left lingual gyrus (0.0601). When subjects were doing the visual task, connectivity was the highest inthe right superior parietal gyrus (0.0684), followed by the left middle occipital gyrus (0.0653). L.CAL: Left calcarine fissure and surrounding cortex; R.CAL: right calcarine fissure and surrounding cortex; L.CUN: left cuneus; R.CUN: right cuneus; L.LING: left lingual gyrus; R.LING: right lingual gyrus; L.SOG: left superior occipital gyrus; R.SOG: right superior occipital gyrus; L.MOG: left middle occipital gyrus; R.MOG: right middle occipital gyrus; L.IOG: left inferior occipital gyrus; R.IOG: right inferior occipital gyrus; L.FFG: left fusiform gyrus; R.FFG: right fusiform gyrus; L.SPG: left superior parietal gyrus; R.SPG: right superior parietal gyrus; L.ITG: left inferior temporal gyrus; R.ITG: right inferior temporal gyrus.

Table 3 Distribution of resting-state and task-state visual brain regions

Node	Brain regions	Resting-state module	Node	Brain regions	Task-state module
43	L.CAL	5	44	R.CAL	2
44	R.CAL	5	54	R.IOG	2
45	L.CUN	5	56	R.FFG	2
46	R.CUN	5	90	R.ITG	2
47	L.LING	5	52	R.MOG	3
48	R.LING	5	45	L.CUN	4
49	L.SOG	5	46	R.CUN	4
50	R.SOG	5	48	R.LING	4
51	L.MOG	5	49	L.SOG	5
52	R.MOG	5	50	R.SOG	5
53	L.IOG	5	53	L.IOG	5
54	R.IOG	5	59	L.SPG	5
55	L.FFG	5	60	R.SPG	5
56	R.FFG	5	43	L.CAL	6
59	L.SPG	5	47	L.LING	6
60	R.SPG	5	51	L.MOG	6
89	L.ITG	5	55	L.FFG	6
90	R.ITG	5	89	L.ITG	6

L.CAL: Left calcarine fissure and surrounding cortex; R.CAL: right calcarine fissure and surrounding cortex; L.CUN: left cuneus; R.CUN: right cuneus; L.LING: left lingual gyrus; R.LING: right lingual gyrus; L.SOG: left superior occipital gyrus; R.SOG: right superior occipital gyrus; L.MOG: left middle occipital gyrus; R.MOG: right middle occipital gyrus; L.IOG: left inferior occipital gyrus; R.IOG: right inferior occipital gyrus; L.FFG: left fusiform gyrus; R.FFG: right fusiform gyrus; L.SPG: left superior parietal gyrus; R.SPG: right superior parietal gyrus; L.ITG: left inferior temporal gyrus; R.ITG: right inferior temporal gyrus; L: left; R: right.

BOLD signals were higher during the complex task in which the peak voxel [–12, –93, 30] was located at BA19. The voxels at BA18 [–6, –9, 36] were selected to construct ROIs, and the fMRI signals were compared. As shown in **Figure 3D**, BA18 was slightly activated during the complex task. This indicates that the visual cortex was activated first in the visual tasks, and the stimuli features were identified through the integration and processing of image information in the frontal lobe.

Brain-function network and attributes

Fischer-Z value of the correlation coefficients in the vision-related brain regions

The correlation coefficients between voxels in visual brain regions were subjected to Fisher-*Z* transformation to ensure a normal distribution.

At rest, 18 brain regions involving 162 connecting lines contributed to visual information processing. *Z*-values were analyzed using a *t*-test and 84 positive connections were obtained. When $|Z| \geq 0.2$, there were 23 positive connections, when $0.2 > |Z| \geq 0.15$, there were 3 positive connections, when $0.15 > |Z| \geq 0.1$, there were 6 positive connections, and when $0.1 > |Z| \leq 0.05$, there were 13 positive connections. When $|Z| \leq 0.05$, 18 brain regions involving 45 positive connections critically contributed to visual information processing (**Figure 4A**).

When subjects viewed stimuli with different color and shape features, 18 brain regions containing 162 lines were shown to be involved in visual information processing. Transformed *Z*-values were analyzed using a *t*-test and 86 positive connections were found. When $|Z| \geq 0.2$, there were

22 positive connections, when $0.2 > |Z| \geq 0.15$, there were 8 positive connections, when $0.15 > |Z| \geq 0.1$, there were 14 positive connections, and when $0.1 > |Z| \geq 0.05$, there were 21 positive connections, When $|Z| \geq 0.05$, 18 brain regions involving 65 positive connections critically contributed to visual information processing (**Figure 4B**).

Node connectivity in the vision-related brain regions

Connectivity refers to the total number of effective connections at a certain node in the brain network and evidences the importance of this node in the network.

During the visual task, 18 brain regions were highly involved in visual information processing. From high to low connectivity, they were as follows: right superior parietal gyrus (0.0684), left middle occipital gyrus (0.0653), left lingual gyrus, right middle occipital gyrus, right precuneus, right superior occipital gyrus, left inferior occipital gyrus, left inferior occipital gyrus, left calcarine fissure and surrounding cortex, right inferior occipital gyrus, left precuneus, right inferior temporal gyrus, left superior parietal gyrus, left fusiform gyrus, right calcarine fissure and surrounding cortex, right lingual gyrus, right fusiform gyrus, and left inferior temporal gyrus (**Figure 5**).

When subjects were at rest, 18 brain regions were highly involved in visual information processing. From high to low connectivity, they were as follows: left middle occipital gyrus (0.0621), left lingual gyrus (0.0621), right fusiform gyrus, left superior occipital gyrus, left inferior occipital gyrus, right precuneus, right superior occipital gyrus, left calcarine fissure and surrounding cortex, left precuneus, right lingual gyrus, right inferior temporal gyrus, right middle occipital gyrus, right inferior occipital gyrus, left fusiform gyrus, right calcarine fissure and surrounding cortex, left superior parietal gyrus, right superior parietal gyrus, and left inferior temporal gyrus (**Figure 5**).

Module partition of the brain-function network

The resting-state brain-function network was divided into six modules, and the vision-related brain regions were located in module 5 (**Figure 6A**). Those in the module included: left and right calcarine fissure and surrounding cortex (No. 43 and 44 in the AAL template), left and right cuneus (No. 45 and 46 in the AAL template), left and right lingual gyrus (No. 47 and 48 in the AAL template), left and right superior occipital gyrus (No. 49 and 50 in the AAL template), left and right middle occipital gyrus (No. 51 and 52 in the AAL template), left and right inferior occipital gyrus (No. 53 and 54 in the AAL template), left and right fusiform gyrus (No. 55 and 56 in the AAL template), left and right superior parietal gyrus (No. 59 and 60 in the AAL template), as well as left and right inferior temporal gyrus (No. 89 and 90 in the AAL template). Previous studies have shown that the parietal lobe is responsible for the binding of color and shape features, while the fusiform gyrus is associated with the processing of color and shape features.

The task-state brain-function network was divided into seven modules and the vision-related brain regions were located in different modules (**Figure 6B**). Among them, the right calcarine fissure and surrounding cortex (No. 44 in the AAL template), right inferior occipital gyrus (No. 54 in AAL template), right fusiform gyrus (No. 56 in AAL template), and right inferior temporal gyrus (No. 90 in the AAL template) were located in module 2. The right middle occipital gyrus (No. 52 in the AAL template) was located in module 3. The left and right cuneus (No. 45 and 46 in the AAL template) and right lingual gyrus (No. 48 in the AAL template) were located in module 4. The left and right superior occipital gyrus (No. 49 and 50 in the AAL template), left inferior occipital gyrus (No. 53 in the AAL template), and left and right superior parietal gyrus (No. 59 and 60 in the AAL template) were located in module 5. The left calcarine fissure and surrounding cortex (No. 43 in the AAL template), left lingual gyrus (No. 47 in the AAL template), left middle occipital gyrus (No. 51 in the AAL template), left fusiform gyrus (No. 55 in the AAL template), and left inferior temporal gyrus were located in module 6. The module distribution of resting-state and task-state visual brain regions is shown in **Table 3**.

Discussion

Position of activated regions

Vision-related brain regions were significantly activated in two conditions. The presence of activation and the degree of activation supported the theory regarding ventral visual information processing pathway (Saur et al., 2008). The ventral visual pathway extends from the primary visual cortex to the occipital-temporal cortex through visual association cortex.

Brain activation during color and shape recognition may increase along with the number of visual features. Here, increased complexity promoted the activation of brain regions. Simple tasks will not mobilize the frontal lobe. This is consistent with the findings of Smith and Jonides (1997), which showed right prefrontal lobe and BA46 activation using PET scans. The frontal lobe plays a role in the feature integration process and the right prefrontal lobe is highly involved in the processing of visual materials. BA7 is also responsible for the integration of visual spatial information, and receives projections from the corpus striatum and cingulate gyrus.

Analysis of brain functional network

Z values of visual brain regions

The complex brain network associated with the vision was also active even at rest when no visual tasks were being performed.

The results of the present study showed that there were 18 nodes involving 162 pairs of functional connections in the vision-related brain network. There were 84 and 86 pairs of positive connections found at rest and during the task, respectively. When the minimum threshold value was defined as 0.05, 45 and 65 pairs of positive connections were found at rest and during the task, respectively. This indicates that connections between the visual brain regions were sparse during the resting state, but became dense during the task.

Our findings further confirmed the dynamic equilibrium of the brain network, in which sparse connections during

a resting state maintain a state of readiness for use in executing tasks. Once a visual task begins, the brain-function network immediately enters a state of tight connections, and brain regions with similar functions begin to strengthen functional connections, allowing color and shape processing, and ultimately achieving the binding of color and shape.

Connectivity of visual brain regions

The connectivity in the left middle occipital gyrus and the left lingual gyrus was higher during both resting and task states, with only a subtle difference between states. At rest, the left middle occipital gyrus and left lingual gyrus had the first and second highest connectivity values, while during the task, they had the second and third highest connectivity. Therefore, the left middle occipital gyrus and the left lingual gyrus are the crucial and stable nodes in the vision-related brain network.

Bundling of visual features is achieved through the spatial position, and attention to the same position leads to binding of visual components at this position. In the two-stage theory of feature binding, the binding of surface features such as color and shape is classified as the second stage of the two-stage process. At this stage, binding requires attention and the parietal lobe plays a key role. Increasing evidence has shown a correlation between parietal lobe activity and spatial attention (Haxby et al., 1991; Humphreys et al., 2000; Marois et al., 2000). When the resting state transitions to the task state, the degree of the connectivity in the left and right parietal lobe is increased. This can be explained by the fact that the parietal lobe is highly involved in the execution of the color and shape binding, which needs the information from other brain regions.

Mounting evidence has demonstrated that the fusiform gyrus is responsible for the color processing, and it can filter excessive information and process some static shapes. The inferior temporal gyrus is mainly involved with shape-related information, and can filter out useless information and transmit shape information to advanced visual areas. For instance, inferior temporal cortex (TI) or fusiform gyrus (GF) injury result in disorders of shape identification (Walsh and Butler, 1996; Merigan et al., 1997). A large number of studies regarding brain cognitive imaging techniques (MEG, PET, fMRI) have demonstrated that the inferior temporal gyrus is responsible for shape perception (Kraut et al., 1997; Kourtzi and Kanwisher, 2000; Okusa et al., 2000). In color and shape binding experiments, the inferior temporal gyrus was critically involved in color and shape processing and filtering unrelated information, was only connected to the advanced brain regions that were related to vision, and ultimately transferred information to advanced brain regions. Therefore, connectivity of the fusiform gyrus and inferior temporal gyrus during the task-state was reduced compared with the resting state.

Module partition analysis

At rest, all visual brain regions were located in module 5. This indicates that brain regions with similar functions were tightly connected during the resting state, while those with different functions were sparsely connected. Additionally, hearing and language involved separate brain function networks.

During the task, module 2, 5, and 6 is analyzed first. Increasing evidence shows that the brain has four parallel systems for the processing visual information: V5 is responsible for motor information, V4 is responsible for color information. Both V3 and V4 are responsible for shape information, with V3 responding to dynamic shape and V4 responding to static shape. The right calcarine fissure and surrounding cortex within module 2 are the primary visual cortex (V1), which functions to accept external sensory information and transfer it to higher visual cortical regions. The right inferior occipital gyrus is responsible for color processing, the right fusiform gyrus mainly deals with color information and static shape information, and the right inferior temporal gyrus is involved in advanced visual processing. Module 6 includes the left calcarine fissure and surrounding cortex, left lingual gyrus, left middle occipital gyrus, left fusiform gyrus, and left inferior temporal gyrus. The functions of these brain regions are similar to that of the left regions in module 2. Module 5 includes the right superior occipital gyrus, left inferior occipital gyrus, and left and right superior parietal gyri. Module 2 and 6 confirm the ventral pathway along the occipital and temporal lobe is associated with color and shape processing.

Resting-state brain-function networks have been applied in disease research, but the task-state brain-function network for color and shape binding has not been a common focus of research. This study analyzed a complex network with graph theory and partitioned the brain-network modules with a community-partitioning algorithm. The hierarchical structure and attributes of the constructed network were analyzed. Understanding the feature-binding process will help establish computer models of vision, and improve image recognition technology.

Author contributions: *YLY designed the study and drafted the manuscript. HXD supervised the manuscript. GYX analyzed experiment data. LXX provided and integrated experimental data. HFL was responsible for the funds and instructing the study. All authors approved the final version of the paper.*
Conflicts of interest: *None declared.*

References

Bracci S, Ietswaart M, Peelen MV, Cavina-Pratesi C (2010) Dissociable neural responses to hands and non-hand body parts in human left extrastriate visual cortex. J Neurophysiol 103:3389-3397.

Cavina-Pratesi C, Kentridge R, Heywood CA, Milner AD (2010) Separate dhannels for processing rorm, texture, and color: evidence from fMRI adaptation and visual object agnosia. Cereb Cortex 20:2319-2332.

Clauset A, Newman ME, Moore C (2004) Finding community structure in very large networks. Phys Rev E Stat Nonlin Soft Matter Phys 70:066111.

Cordes D, Haughton V, Carew JD, Arfanakis K, Maravilla K (2002) Hierarchical clustering to measure connectivity in fMRI resting-state data. J Magn Reson Imaging 20:305-317.

Eguiluz VM, Chialvo DR, Cecchi GA, Baliki M, Apkarian AV (2005) Scale-free brain functional networks. Phys Rev Lett 94:018102.

Ferrarini L, Veer IM, Baerends E, van Tol MJ, Renken RJ, van der Wee NJA, Veltman DJ, Aleman A, Zitman FG, Penninx B, van Buchem MA, Reiber JHC, Rombouts S, Milles J (2009) Hierarchical functional modularity in the resting-state human brain. Hum Brain Mapp 30:2220-2231.

Guo H, Chen C, Cao XH, Xiang J, Chen JJ, Zhang KR (2014) Resting-state functional connectivity abnormalities in first-onset unmedicated depression. Neural Regen Res 9:153-163.
Haxby JV, Grady CL, Horwitz B, Ungerleider LG, Mishkin M, Carson RE, Herscovitch P, Schapiro MB, Rapoport SI (1991) Dissociation of object and spatial visual processing pathways in human extrastriate cortex. Proc Natl Acad Sci U S A 88:1621-1625.
Haxby JV, Gobbini MI, Furey ML, Ishai A, Schouten JL, Pietrini P (2001) Distributed and overlapping representations of faces and objects in ventral temporal cortex. Science 293:2425-2430.
He Y, Wang JH, Wang L, Chen ZJ, Yan CG, Yang H, Tang HH, Zhu CZ, Gong QY, Zang YF, Evans AC (2009) Uncovering intrinsic modular organization of spontaneous brain activity in humans. PLoS One 4:e5226.
Hilgetag CC, Burns GA, O'Neill MA, Scannell JW, Young MP (2000) Anatomical connectivity defines the organization of clusters of cortical areas in the macaque and the cat. Philos Trans R Soc Lond B Biol Sci 355:91-110.
Humphreys GW, Cinel C, Wolfe J, Olson A, Klempen N (2000) Fractionating the binding process: neuropsychological evidence distinguishing binding of form from binding of surface features. Vision Res 40:1569-1596.
Kourtzi Z, Kanwisher N (2000) Cortical regions involved in perceiving object shape. J Neurosci 20:3310-3318.
Kraut M, Hart J, Soher BJ, Gordon B (1997) Object shape processing in the visual system evaluated using functional MRI. Neurology 48:1416-1420.
Liang X, Wang JH, Yan CG, Shu N, Xu K, Gong GL, He Y (2012) Effects of different correlation metrics and preprocessing factors on small-world brain functional networks: a resting-state functional MRI study. PLoS One 7:e32766.
Marois R, Chun MM, Gore JC (2000) Neural correlates of the attentional blink. Neuron 28:299-308.
Merigan W, Freeman A, Meyers SP (1997) Parallel processing streams in human visual cortex. Neuroreport 8:3985-3991.
Meunier D, Achard S, Morcom A, Bullmore E (2009) Age-related changes in modular organization of human brain functional networks. Neuroimage 44:715-723.
Newman ME (2004a) Detecting community structure in networks. Eur Phys J B 38:321-330.
Newman ME (2004b) Fast algorithm for detecting community structure in networks. Phys Rev E Stat Nonlin Soft Matter Phys 69:066133.
Newman ME, Girvan M (2004) Finding and evaluating community structure in networks. Phys Rev E Stat Nonlin Soft Matter Phys 69:026113.
Okusa T, Kakigi R, Osaka N (2000) Cortical activity related to cue-invariant shape perception in humans. Neuroscience 98:615-624.
Saur D, Kreher BW, Schnell D, Kummerer D (2008) Ventral and dorsal pathways for language. Proc Natl Acad Sci U S A 105:18035-18040.
Seo EH, Lee DY, Lee JM, Park JS, Sohn BK, Lee DS, Choe YM, Woo JI (2013) Whole-brain functional networks in cognitively normal, mild cognitive impairment, and alzheimer's disease. PLoS One 8:e53922.
Smith EE, Jonides J (1997) Working memory: a view from neuroimaging. Cogn Psychol 33:5-42.
Song J, Desphande AS, Meier TB, Tudorascu DL, Vergun S, Nair VA, Biswal BB, Meyerand ME, Birn RM, Bellec P, Prabhakaran V (2012) Age-related differences in test-retest reliability in resting-state brain functional connectivity. PLoS One 7:e49847.
Tzourio-Mazoyer N, Landeau B, Papathanassiou D, Crivello F, Etard O, Delcroix N, Mazoyer B, Joliot M (2002) Automated anatomical labeling of activations in spm using a macroscopic anatomical parcellation of the MNI MRI single-subject brain. Neuroimage 15:273-289.
Walsh V, Butler SR (1996) The effects of visual cortex lesions on the perception of rotated shapes. Behav Brain Res 76:127-142.
Walther DB, Caddigan E, Fei-Fei L, Beck DM (2009) Natural scene categories revealed in distributed patterns of activity in the human brain. J Neurosci 29:10573-10581.
White S, Smyth P (2005) A spectral clustering approach to finding communities in graphs. Philadelphia: Siam.
Yu QB, Allen EA, Sui J, Arbabshirani MR, Pearlson G, Calhoun VD (2012) Brain connectivity networks in schizophrenia underlying resting state functional magnetic resonance imaging. Curr Top Med Chem 12:2415-2425.
Yuan YX, Jiang X, Zhu DJ, Chen HB, Li KM, Lv PL, Yu X, Li XJ, Zhang S, Zhang T, Hu XT, Han JW, Guo L, Liu TM (2013) Meta-analysis of functional roles of DICCCOLs. Neuroinformatics 11:47-63.

Copyedited by Phillips A, Norman C, Wang J, Yang Y, Li CH, Song LP, Zhao M